Assessment of Flutter Prediction and Trends in the Design of Large-Scale Wind Turbine Rotor Blades

UT Dallas Author(s):

D. Todd Griffith
Mayank Chetan

Citation:

Griffith, D. T., and M. Chetan. 2018. "Assessment of flutter prediction and trends in the design of large-scale wind turbine rotor blades." Journal of Physics: Conference Series 1037: art. 042008, doi:10.1088/1742-6596/1037/4/042008

IOP Conf. Series: Journal of Physics: Conf. Series **1037** (2018) 042008 doi:10.1088/1742-6596/1037/4/042008

Assessment of flutter prediction and trends in the design of large-scale wind turbine rotor blades

D Todd Griffith[1] **and Mayank Chetan**[1]
[1]Department of Mechanical Engineering, University of Texas at Dallas, Richardson TX 75080, USA
E-mail: tgriffith@utdallas.edu

Abstract. With the progression of novel design, material and manufacturing technologies, the wind energy industry has successfully produced larger and larger wind turbine rotor blades while driving down the levelized cost of energy (LCOE). Though the benefits of larger turbine blades are appealing, larger blades are prone to instabilities due to their long and slender nature, and one of the concerning aero-elastic instabilities of these blades is classical flutter. In this work we assess classical flutter prediction tools for predicting flutter speeds in the design of large blades. Flutter predictions are benchmarked against predictions of previous studies. Then, we turn to the main focus of the study, which is a design to mitigate flutter. Trends in flutter speeds and flutter mode shapes are examined for a series of 100-meter blade designs. Then, a sensitivity study is performed to assess the impacts of blade design choices (e.g. materials choice and material placement) on flutter speed in a redesign study of a lightweight 100-meter blade with small flutter margin. A new design is developed to demonstrate the ability to increase the flutter speed while reducing blade mass through structural design.

1. Introduction

Traditionally flutter speeds are evaluated as one of the final analyses in the design of blades, where using high-fidelity methods like CFD is possible. But with the shift in the market towards larger wind turbine rotors there is a need for a low- to mid-fidelity tool that can be efficiently integrated into the early stages of the design process to ascertain the influence of structural parameters on the onset of flutter. Previous work by Hansen [1] discusses stall-induced vibrations that are inherent to stall-induced wind turbines, additionally Hansen approached the issue by modelling the complete rotor and tower. Lobitz [2] approached the problem of flutter in MW-sized wind turbines with a NASTRAN-based beam finite element model with Theodorsen unsteady aerodynamics [3] for a blade rotating in still air (where the inflow component of wind velocity is neglected and only the rotor plane blade velocity is included). Pourazarm et al [4] have developed and validated a flutter model against previous work with good confidence, using a blade model that accounts for flapwise and torsional degrees of freedom, although the edgewise degree of freedom was neglected in their formulation.

Owens et al [5] developed the BLAST tool, which was similar to the approach of Lobitz, but with an improved structural model. Modifications were made to the mass, stiffness and damping matrices to account for aerodynamic effects, and rotational effects such as Coriolis effects and spin softening. Hansen et al [6] further developed a full turbine model in still air using an eigenvalue approach based on a beam finite element (FE) model with aerodynamic loads modelled using the blade element momentum (BEM) theory coupled with Leishman-Beddoes Dynamic stall model. They concluded that there was a reasonable similarity between flutter predictions for a full turbine versus analysis of an isolated blade uncoupled from the tower.

The over-arching goal of this work is to develop improved low- to mid-fidelity flutter prediction tools that are accurate for and amenable to predicting flutter in the early stages of the design process for large wind turbine blades. As for tool development and assessment, we start with the classical flutter prediction tool, evaluate key assumptions, and benchmark the tool with other studies. After assessing the suitability of the flutter prediction tool, we move to analysis of trends in flutter speeds in the design of large blades (100 meters), which is the main focus of the paper. We investigate the sensitivity and trends of flutter predictions, including the flutter speeds and flutter mode shapes, with respect to blade mass and blade span-wise properties for a series of 100-meter blades. Finally, a design study is performed to evaluate flutter mitigation solutions inspired by the trends study. A re-designed updated 100-meter blade design is presented with improved flutter speed and lower blade mass while still satisfying design requirements for strain, deflection, buckling and fatigue.

2. Theoretical Foundation of the Flutter Prediction Tool

The structural representation of the flutter prediction tool is based on a three-dimensional implementation of Euler-Bernoulli beam finite element, which allows for modelling of all blade deformations including flapwise, edgewise, and torsional components.

For a blade, the system of equations with rotational effects such as Coriolis and spin softening, takes the form

$$M\ddot{x} + \big(D + G(\Omega)\big)\dot{x} + \big(K(x) - S(\Omega)\big)x = F_{\text{cent}}(\Omega) + F \tag{1}$$

Here *M*, *D*, *K* are the mass, damping and stiffness matrices of the blade section respectively. *G(Ω)* introduces the Coriolis matrix and S(Ω) represents the spin softening effects at an angular velocity of *Ω*.

For aerodynamic effects, Theodorsen unsteady aerodynamic theory is introduced and the lift and moment causing the flapping and twisting motion at the defined cross-sections are given by

$$L = \pi\rho b^2\left[\ddot{z} + V\dot{\theta} - ba\ddot{\theta}\right] + 2\pi\rho VbC(k)\left[\dot{z} + V\theta + b(\tfrac{1}{2} - a)\dot{\theta}\right] \tag{2}$$

$$M = \pi\rho b^2\left[ba\ddot{z} - Vb\left(\tfrac{1}{2} - a\right)\dot{\theta} - b^2\left(\tfrac{1}{8} + a^2\right)\ddot{\theta}\right] + 2\pi\rho Vb^2\left(a + \tfrac{1}{2}\right)C(k)\left[\dot{z} + V\theta + b\left(\tfrac{1}{2} - a\right)\dot{\theta}\right] \tag{3}$$

Here ρ is the air density, *b* is the semi-chord of the airfoil section, *a* is the flexural axis position aft of the mid chord as a fraction of the semi-chord, *z(t)* represents the flapwise motion for the sections, *θ(t)* is the torsional motion of the section and *C(k)* is the Theodorsen Function which models the amplitude and phase lag of the aerodynamic forces acting on the section.

$$\mathrm{C(k)} = F(k) + \mathrm{i}G(k) \tag{4}$$

where $k = \frac{\omega b}{U_\infty}$ is the reduced frequency and depends on the oscillatory motion of the airfoil section, U_∞ represents the free stream velocity, which is modelled for a rotating turbine as a function of distance from the hub axis r given by

$$U_\infty = r\Omega \tag{5}$$

The resulting aerodynamic loads are a function of the angular velocity *Ω* and the frequency *ω*. Now, modelling the aerodynamic mass, damping and stiffness into equation (1) results in

$$(M + M_A(\Omega))\ddot{x} + \big(D + G(\Omega) + D_{\mathrm{A}}(\Omega,\omega)\big)\dot{x} + \big(K(x) - S(\Omega) + K_{\mathrm{A}}(\Omega,\omega)\big)x = F_{\text{cent}}(\Omega) + F_A(\Omega) \tag{6}$$

Where $M_{\mathrm{A}}(\Omega)$, $D_{\mathrm{A}}(\Omega,\omega)$ & $K_{\mathrm{A}}(\Omega,\omega)$ are the aerodynamic mass, damping and stuffiness matrices respectively. Since a modal analysis is to be done, this system can be represented as

$$(M + M_A(\Omega))\ddot{x} + \big(C + G(\Omega) + C_{\mathrm{A}}(\Omega,\omega)\big)\dot{x} + \big(K(x) - S(\Omega) + K_{\mathrm{A}}(\Omega,\omega)\big)x = 0 \tag{7}$$

This method and similar methods have been used reliably in the past for flutter predictions. However, we now consider assumptions of this model. Namely, the main assumptions are: (1) the flow is always attached to the airfoil section, (2) the airfoil is thin, (3) the resulting wake is also flat (parallel to the rotor plane inflow), (4) that the blade rotates in still air, and (5) the wake of the blade does not affect the nearing blade. Assumptions 1, 2, and 3 are assumptions of the Theodorsen theory, which are reasonable assumptions over the majority of the blade span, although Assumptions 1 and 2 can be challenges for large blades with thick airfoils susceptible to flow separation near the blade root.

The still air assumption (Assumption 4) is the major assumption of the flutter prediction procedure and is now considered. Of course, the wind velocity at each span-wise section of the blade depends upon the inflow component to the rotor plus the local in-plane rotor plane component (due to $r\Omega$). The still air assumption considers only the $r\Omega$ component. One way to evaluate the impact of the inflow velocity effect on flutter speed is to directly include it in the model, and this has been performed by Hafeez et al [7] where the Theodorsen function [8] was modified to account for inflow along with the rotor plane velocity. They show that including the inflow resulted in a 5% increase in flutter speed versus the still air assumption. The conclusions are that the inflow has a small effect on flutter speed and that the still air assumption tends to be conservative, thus the still air assumption is a reasonable and acceptable assumption.

In order to further evaluate the impact of the still air assumption, we performed a study with our tool where we varied the pitch angle of the blade. Varying the pitch angle effectively results in a wind velocity having both inflow and $r\Omega$ components. We found similar trends to [7] as the flutter speed increased from 9.84 rpm for 0 degree pitch to 10.04, 10.35, 11.03, and 13.04 rpm for 2, 5, 10, and 20 degrees of blade pitch, which also indicates that the inflow component tends to increase the flutter speed. The other implication of this trend is that in Region 3 (above rated speed) operation, the flutter speed will increase with blade pitch.

3. Description of the Wind Turbine Blades Analyzed in This Study

For the preliminary verification of the flutter tool, five blade models are studied; NREL 5MW [9] and the SNL 100-meter blade series including SNL100-00 13.2MW [10], SNL100-01 13.2MW [11], SNL100-02 13.2MW [12] and SNL100-03 13.2MW [13]. The NREL 5MW offshore wind turbine was designed to be used as a baseline representing utility grade offshore wind turbines. The SNL100-00 blade (for a 13.2MW turbine) is an all-glass 100-meter blade developed at Sandia National Laboratories, this blade was designed to be a baseline for large wind turbine blade design studies. The SNL100-01 blade was designed based on the SNL100-00 baseline, but with a carbon spar cap. The SNL100-02 blade further reduced the weight of the SNL100-01 blade, attributed to the use of advanced core materials in its design. The SNL100-03 blade, the fourth and final design in the series, involved a significant change in geometry and materials. In this design, flatback airfoils were incorporated instead of sharp trailing edge airfoils and a completely new aerodynamic design was developed. From SNL100-00 to SNL100-03, this resulted in a 56% weight reduction for the entire SNL 100-meter series. A summary of the properties of the blades are represented in table 1.

Table 1. Geometry and operating specification of the blade models examined in the study.

Blade	Length (m)	Maximum Chord (m)	Mass (kg)	Rated Power (MW)	Rated Speed (rpm)
NREL 5MW	61.50	4.60	17,740	5.00	12.10
SNL100-00	100.00	7.628	114,172	13.2	07.44
SNL100-01	100.00	7.628	73,995	13.2	07.44
SNL100-02	100.00	7.628	59,047	13.2	07.44
SNL100-03	100.00	5.226	49,519	13.2	07.44

Key span wise properties for the blades are compared in figures 1-6 including flapwise, edgewise, & torsional stiffness, mass per unit length, chord-wise CG, and chord-wise elastic axis offset, respectively.

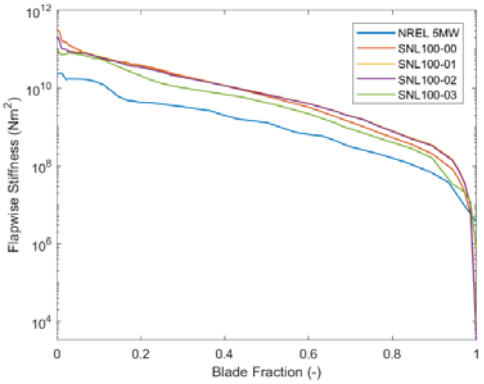

Figure 1. Flapwise Stiffness Distribution.

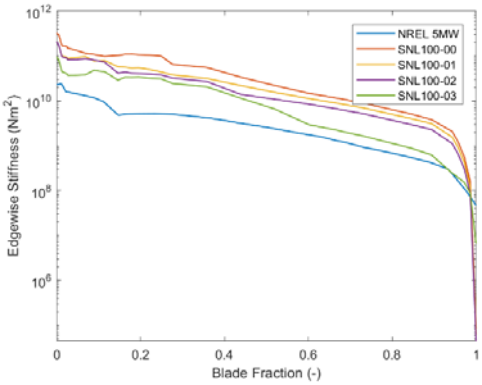

Figure 2. Edgewise Stiffness Distribution.

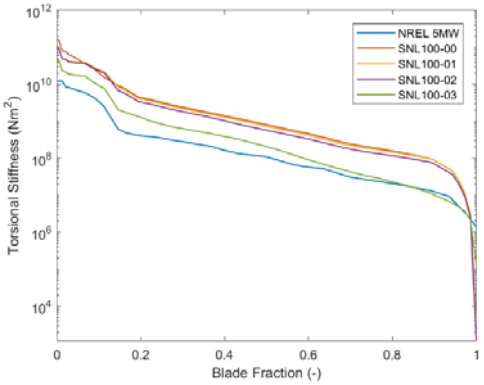

Figure 3. Torsional Stiffness Distribution.

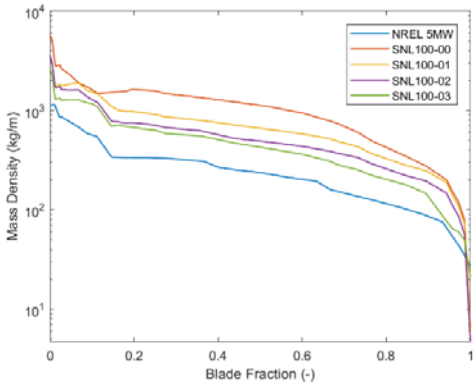

Figure 4. Mass Distribution.

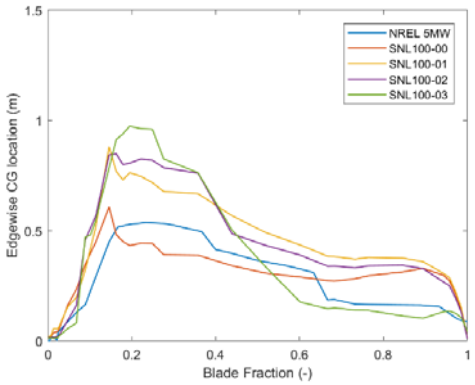

Figure 5 Edge-wise CG Offset Distribution.

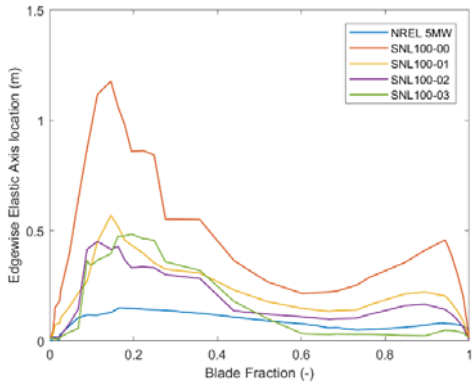

Figure 6. Elastic Axis Offset Distribution.

4. Flutter Tool Benchmarking and Assessment of Flutter Trends

4.1. Benchmarking and verification of flutter tool predictions

As a first step to assess the flutter prediction tool, the blade models discussed in the previous section are analyzed and compared with previous studies. To gain a more thorough understanding, both critical flutter speeds and flutter mode shapes are analyzed. We find generally good agreement in comparing our predictions with those of other studies (as noted in table 2).

The flutter speed for NREL 5MW blade in the current study is 20.02 rpm, which is close to the speed predicted by Pourazarm et al although our tool predicts a different flutter mode (2nd edge-wise coupled with 2nd flapwise mode). The difference in predictions may be attributed to the fact that the edgewise degree of freedom is not considered in Reference [4]. The flutter speeds for the SNL100-XX series of 100 meter blades (SNL100-00, -01, -02, -03) are generally in good agreement with previous studies ([5], [11], [12], [13]) and are on the conservative side. Note that the maximum rpm for the SNL100-XX series is 7.44 rpm and the flutter ratio is calculated for each and placed in parentheses for the current study.

Table 2. The flutter speeds in units of rpm: Current study and previous studies for all blade models.

Blade	Pourazarm *et al*	Hansen	Owens *et al*	Griffith *et al*	Current Study (Margin)
NREL 5MW	20.70	24.00			20.02 (1.65)
SNL100-00	16.91		13.05		14.44 (1.94)
SNL100-01				13.69	12.81 (1.72)
SNL100-02				12.72	11.64 (1.56)
SNL100-03				10.41	09.84 (1.32)

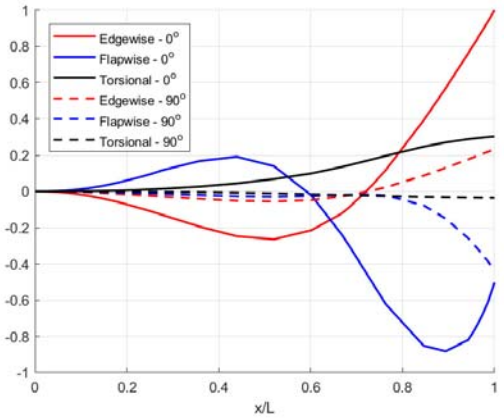

Figure 7. Flutter mode for SNL100-00.

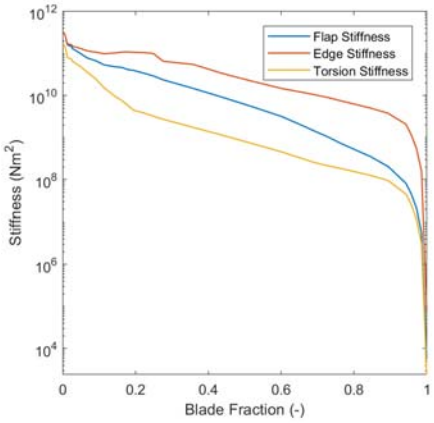

Figure 8. Stiffness Distribution for SNL100-00.

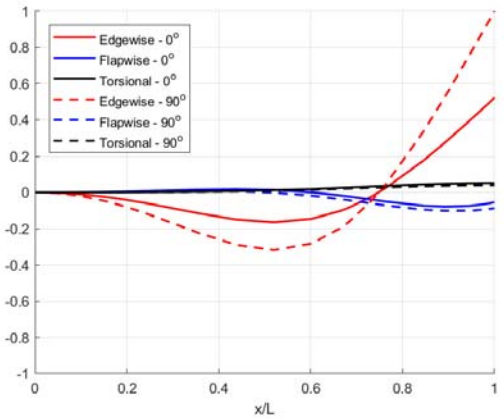

Figure 9. Flutter mode for SNL100-01.

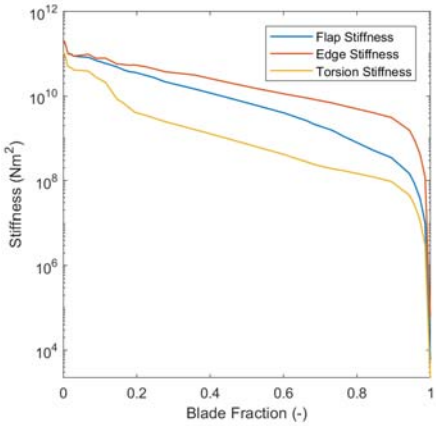

Figure 10. Stiffness Distribution for SNL100-01.

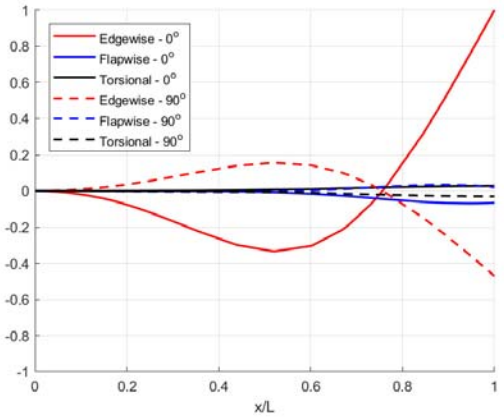

Figure 11. Flutter mode for SNL100-02.

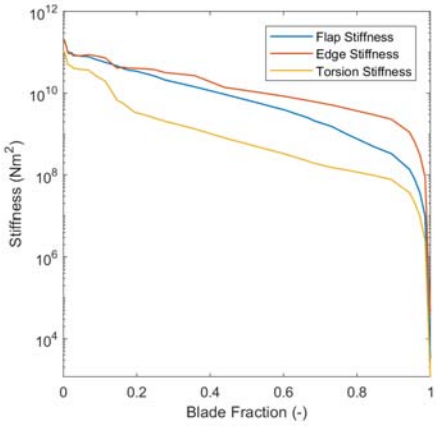

Figure 12. Stiffness Distribution for SNL100-02.

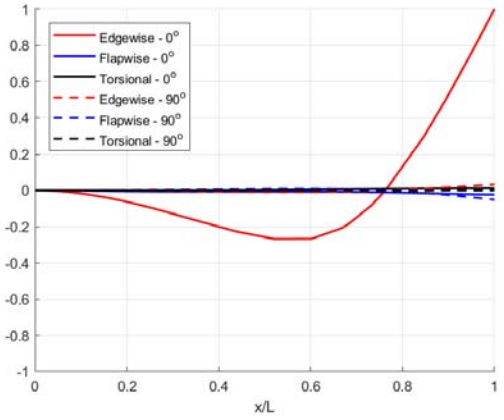

Figure 13. Flutter mode for SNL100-03.

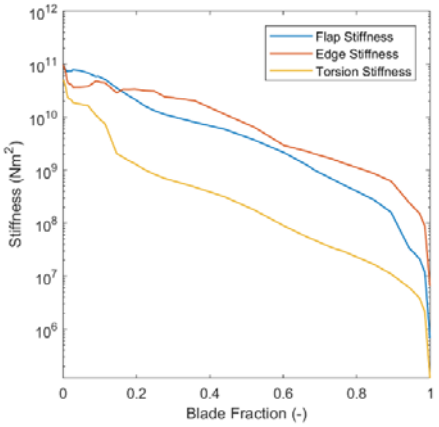

Figure 14. Stiffness Distribution for SNL100-03.

4.2. Analysis of trends in the flutter speeds and flutter mode shapes for the SNL100-XX series

We now examine trends in the flutter predictions for the SNL100-XX blade series (SNL100-00, SNL100-01, SNL100-02, and SNL100-03). First we note the trend to lower flutter speed (and lower flutter ratio) of the 100-meter designs as the mass of the designs was reduced. Note from Table 2 that for the SNL100-XX series the flutter speeds (rpm) are 14.44, 12.81, 11.64, and 9.84 and the flutter margins are shown in parentheses as 1.94, 1.72, 1.56, and 1.32. The trend in reduced flutter speed is clear for the first three blades, which have the same airfoils and aerodynamic design, and this trend continues for the most lightweight SNL100-03 design, which was redesigned aerodynamically with a significantly smaller chord using flatback airfoils. In reviewing the span-wise stiffness properties, the trend to lower flapwise, edgewise and torsional stiffnesses is evident and this the main driver of reduced flutter speed in the SNL100-XX series. Clearly, the flutter margin for SNL100-03 is close to a critical value at only 32% above the max (rated) rpm.

We now examine the flutter mode shapes for the SNL100-XX series. In studying the flutter mode shapes for these large turbine blades, we observed an edgewise and flapwise coupled flutter mode in the SNL100-00 blade – figure 7, in the subsequent generations of the SNL100-XX series blades the flapwise contribution in the mode shape decreases. As we continue to the SNL100-03 blade – figure 13, there is a significantly greater edgewise contribution, this correlates to the decreasing edgewise stiffness as observed in figure 14, in comparison to the other stiffness components. Thus, the principal trend in the mode shapes for this blade series is growing importance of the edgewise coupled flutter mode versus the more traditional flapwise coupled flutter mode. As designers, we note this is a very serious concern because the edgewise (in-plane) aerodynamic damping is relatively very low compared to flapwise

aerodynamic (out of plane) damping. And, the in-plane modes can be excited by in-plane rotor loads including gravitational and inertial effects.

4.3. Trends in CG offset, AC and EA Offset for the analyzed wind turbine blades

In addition to the stiffness distribution along the span, the chordwise location of the elastic axis (EA), mass center (CG) and the aerodynamic center (AC) of the blade contributes to the flutter performance of the blade. In blade design the elastic axis are adjusted so that they align with the reference or pitch axis of the blade.

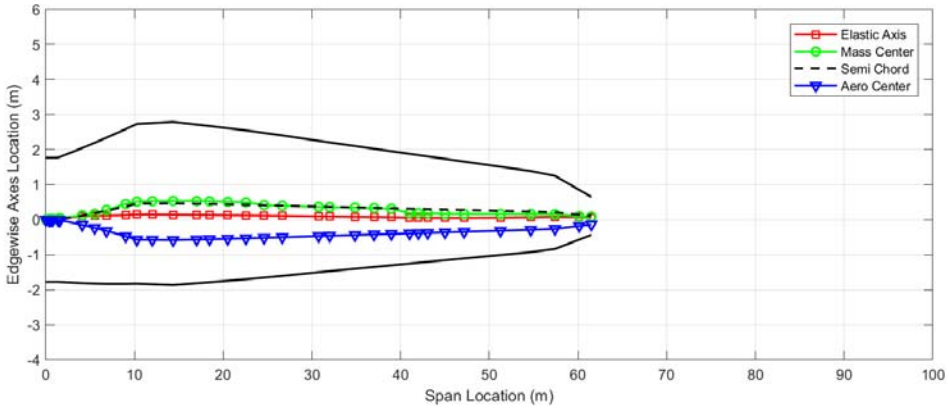

Figure 15. Location of Structural characteristics for NREL 5MW blade.

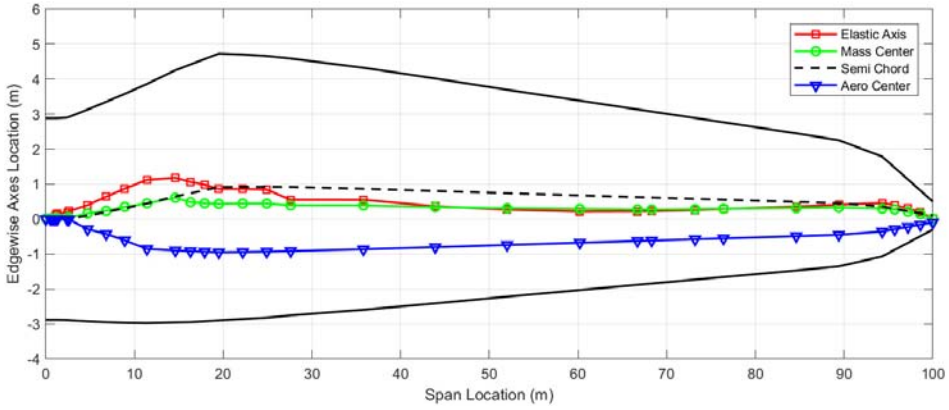

Figure 16. Location of Structural characteristics for SNL100-00 blade.

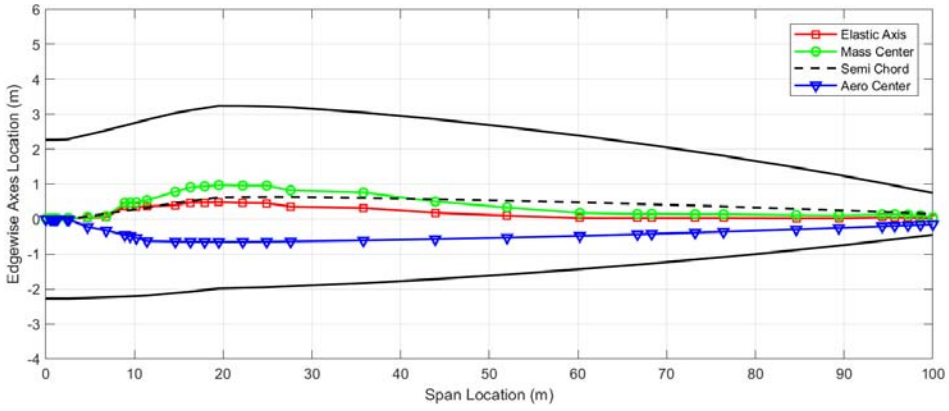

Figure 17. Location of Structural characteristics for SNL100-03 blade.

5. Blade Redesign to Improve Flutter Margin: Design of UTD100-04 100-meter Blade

In this section we explore a structural redesign of the SNL100-03 blade, which was predicted to have a flutter speed only 32% above the maximum operating rpm. Through a design study, we investigate the impact of material placement and material selection on the flutter speed while continuing to comply with other requirements from industry design standards.

5.1. Design Strategy for Improved Flutter Speeds for UTD100-04

From the previous section we observed that the edgewise stiffness is a driving factor for the onset of flutter in these large blades. An intuitive approach to the problem would be to increase one or both the edgewise and torsional stiffness that would result in either an increase in flutter speed or a change in the dominant or characteristic flutter mode. In order to increase the edgewise stiffness, we consider modifications to the trailing edge reinforcement that is already designed into SNL100-03. Secondly, we consider adding leading edge reinforcement. The strategy we propose to mitigate flutter through structural design is as follows: increase the edgewise stiffness through trailing edge and/or leading edge reinforcement while managing the chord-wise CG and EA offsets and ensuring that in-plane (edge-wise) fatigue life for the blade under gravitational loading is adequate.

5.2. Design requirements and analysis

For the design of wind turbine blades the bounding load conditions are considered from the IEC design load cases for a class 1B site [14]. The evaluation of ultimate strength, deflection, fatigue and buckling stability is done using the Germanischer Lloyd (GL) partial safety factors [15] which calculated for combined load and material partial safety factors. The resulting allowable values, which were the same as those for design of SNL100-003, are noted in table 3.

Table 3. Blade Design Allowable.

Analysis	Metric allowable
Ultimate Strain	Max strain = 5139 micro-strain
Deflection	13.67m
Buckling Factor	2.042
Fatigue Life	20 Years

The SNL13.2-00-Land [16] based wind turbine model is used to run the FAST [17] simulations for the various new blade design options. Additionally, the blade is analyzed in the finite element package ANSYS to evaluate buckling and detailed stresses and strains. This design does not modify the root build-up of SNL100-03 blade and thus maintaining a similar platform for mounting the blade to the rotor. Because the UTD100-04 blade was not aerodynamically redesigned, the same extreme load case was used for bucking calculations. We report the frequency of buckling mode, which provides the scaling factor for the applied load in the calculation would result in buckling.

5.3. Flutter performance of redesigned UTD100-04 Blade for various flutter mitigations

Following the strategy developed and noted above, the leading edge (LE) and trailing edge (TE) reinforcements were modified and the flutter speeds evaluated. For the LE, uni-axial composite (Uni), double biased composite (DB), tri-axial composite (Triax), and carbon fiber composite (Carbon) layers were evaluated, these updates showed an increased flutter performance attributing to the increase in the edgewise stiffness and the chordwise CG moving towards the LE as noted in table 4. Next, the already existing TE reinforcement was changed from Uni glass to Uni Carbon, this resulted in a decrease in flutter speed due to the elastic axis moving aft. Finally, the double biased LE reinforcement was combined with the carbon TE resulting in an improvement in the flutter speed and decrease the mass, which is presented as a normalized value with respect to the baseline.

Table 4. Structural design variations considered to increase flutter speed for UTD100-04.

Modification	Specifics	Flutter Speed (RPM)	Frequency (Hz)	Normalised Mass
SNL100-03	Baseline Case	9.84	1.9409	1.0000
LE Reinforcement	Uni 4 Layers	9.88	1.9783	1.0367
LE Reinforcement	Uni 6 Layers	10.05	1.9943	1.0551
LE Reinforcement	DB 4 Layers	11.11	1.9339	1.0341
LE Reinforcement	DB 6 Layers	11.43	1.9287	1.0511
LE Reinforcement	Triax 4 Layers	10.56	1.9568	1.0354
LE Reinforcement	Triax 6 Layers	10.76	1.9624	1.0531
LE Reinforcement	Carbon 4 Layers	10.17	2.1254	1.0233
TE Reinforcement	Uni → Carbon	9.24	1.9777	0.9235
LE DB 4 Layer + Carbon TE	-	10.54	1.9703	0.9575
LE DB 6 Layer + Carbon TE	-	10.86	1.9642	0.9746

5.4. Final UTD100-04 Performance summary

The updated blade with the 6-layer DB LE reinforcement and carbon TE is selected as our candidate blade as not only does the flutter speed increase but the blade mass is reduced with respect to SNL100-03 as evident in table 4. After a few design changes to satisfy buckling requirements, the blade satisfied the design criteria set forth in section 5.2. The maximum tip deflection and max strain is lower than the SNL100-03 blade as the flap, edge, and torsional stiffnesses are higher. The resulting lowest buckling frequencies 2.13 is above the allowable value of 2.042. Table 5 summarizes the operating specifications of the UTD100-04 blade as compared to the SNL100-XX series of 100-meter blades. For the final UTD100-04 design the flutter speed was increased by 10.3% and the mass of the blade is reduced by 1% with respect to the SNL100-03.

Table 5. Geometry and operating specification of the blade models used in the study.

Parameter	SNL100-00	SNL100-01	SNL100-02	SNL100-03	UTD100-04
Airfoil Type	DU (sharp)	DU (sharp)	DU (sharp)	FB (flatback)	FB (flatback)
Blade Length (m)	100	100	100	100	100
Blade Mass (kg)	114,172	73,995	59,047	49,519	49,126
Design Load (kN-m)	110,700	~110,700	~110,700	74,930	74,930
Max Deflection (m)	12.3	10.48	10.51	13.11	<13.11
Flap Fatigue (years)	>>1000	202	182	21	>21
Edge Fatigue (years)	1290	1260	352	77	>77
Buckling (-)	2.173	2.077	2.100	2.05	2.13
Surface Area (m^2)	1262	1262	1262	886	886
Flutter Speed (rpm)	14.44	12.81	11.64	9.84	10.86

6. Concluding Remarks and Future Work

From the study of flutter in wind turbine blades, a pattern emerges of larger blades having lower per-rev flutter speeds. Thus, there is a need for a low- to mid-fidelity tools that can be efficiently integrated into the early stages of the design process to predict flutter. Addressing this need for large blade design is the focus of the present study. Toward this goal, the main contributions of this paper are (1) an assessment of the classical flutter prediction tool, (2) a comprehensive study of the flutter prediction characteristics (flutter speeds and flutter mode shapes) for a series of four 100-meter blades of decreasing mass, (3) a redesign effort to mitigate flutter through structural design of material choice and material placement.

Regarding the flutter prediction tool, we found that our tool is in very good agreement with other works, which we determined from a benchmarking study. We investigated the still air assumption of the flutter tool and, based on other works and our own studies, found that the still air assumption is a reasonable assumption having a small effect yet conservative effect on flutter speed prediction.

Secondly, we performed a comprehensive study of the trends in flutter characteristics as they vary with structural design choices (materials, geometry) for a series of 100-meter blades. The first

observation is that flutter speeds are reduced as blade mass is reduced. This result was shown to be attributed to reduction in blade flapwise, edgewise, and torsional stiffness resulting from the mass reduction. The other observation is that the flutter modes in large turbine blades have a major edgewise contribution in addition to flapwise and torsional components. The prevalence of the edgewise contribution grew as blade mass was reduced in the 100-meter blade series.

Thirdly, the trends study showed the need to address the edgewise flutter modes in large blade design. Thus, a redesign study was performed with a new design strategy proposed for greater stiffening for large blades in the edgewise direction to mitigate the predicted low flutter speed. The lowest mass blade in the 100-meter blade series (SNL100-03) having low flutter speed was redesigned to demonstrate a 10.3% increase in flutter speed along with 1% reduction in blade mass, while continuing to satisfy all design requirements for loads.

A future extension of this work should include comparison of these flutter predictions with aero-elastic codes capable of modelling all the key blade dynamics (including flapwise, edgewise, and torsional motions). Further, the tools should be compared against experimental data. In addition, we envision future modifications to the theoretical foundation to account for characteristics of forthcoming large blade designs for new rotor configurations including downwind effects and highly coned rotors.

7. References

[1] Hansen M H 2007 Aeroelastic instability problems for wind turbines *Wind Energy* **10(6)** pp 551
[2] Lobitz D W 2004 Aeroelastic stability predictions for a MW-sized blade *Wind Energy* **7(3)** pp211
[3] Theodorsen T 1935 General theory of aerodynamic instability and the mechanism of flutter *NACA Report 496* (Washington, D.C.)
[4] Pourazarm P, Modarres-Sadeghi Y and Lackner M 2016 A parametric study of coupled-mode flutter for MW-size wind turbine blades *Wind Energy* **19(3)** pp497-514
[5] Owens B C, Resor B, Griffith D T and Hurtado J 2013 Impact of modeling approach on flutter predictions for very large wind *Proc. of the American Helicopter Society 69th Annual Forum*
[6] Hansen M H 2004 Stability analysis of three-bladed turbines using an eigenvalue approach *Proc 42nd AIAA Aerospace Sciences Meeting and Exhibit* p505
[7] Abdel Hafeez M M and El-Badawy A A 2018 Flutter Limit Investigation for a Horizontal Axis Wind Turbine Blade *J. of Vibration and Acoustics*.
[8] Wendell J 1982 Simplified aeroelastic modeling of horizontal-axis wind turbines *Technical Report DOE/NASA/3303-3, NASA-CR-168109* (Cambridge, USA)
[9] Jonkman J M, Butterfield S, Musial W and Scott G 2009 Definition of a 5-MW reference wind turbine for offshore system development *National Renewable Energy Laboratory Report NREL/TP-500-38060* (Golden, CO)
[10] Griffith D T and Ashwill T D 2011 The Sandia 100-meter All-glass Baseline Wind Turbine Blade: SNL100-00 *Sandia National Laboratories Technical Report SAND2011-3779*
[11] Griffith D T 2013 The SNL100-01 blade: carbon design studies for the Sandia 100-meter blade *Sandia National Laboratories Technical Report SAND2013-1178*
[12] Griffith D T 2013 The SNL100-02 Blade: Advanced Core Material Design Studies for the Sandia 100-meter Blade *Sandia National Laboratories Technical Report* SAND2013-10162
[13] Griffith D T and Richards P W 2014 The SNL100-03 Blade: Design Studies with Flatback Airfoils for the Sandia 100-meter Blade *Sandia National Labs Technical Report SAND2014-18129*
[14] International Electrotechnical Commission (IEC) Design Standard, IEC 61400-1 Ed.3: Wind turbines - Part 1: Design requirements
[15] Germanischer-Lloyd (GL) Design Standard, Guideline for the Certification of Wind Turbines Edition 2010.
[16] Griffith D T and Resor B R 2011 Description of Model Data for SNL13.2-00-Land: A 13.2 MW Land-based Turbine Model with SNL100-00 Blades *Sandia National Laboratories Technical Report, SAND2011-9310P*, December
[17] Jonkman J M and Buhl M L Jr 2004 FAST user's guide *National Renewable Energy Lab, NREL/EL-500-29798* (Golden, CO)